

# The Inverse Drum Machine: Source Separation Through Joint Transcription and Analysis-by-Synthesis

Bernardo Torres, Geoffroy Peeters, Gaël Richard

**Abstract**—We present the Inverse Drum Machine (IDM), a novel approach to Drum Source Separation that leverages an analysis-by-synthesis framework combined with deep learning. Unlike recent supervised methods that require isolated stem recordings for training, our approach is trained on drum mixtures with only transcription annotations. IDM integrates Automatic Drum Transcription and One-shot drum Sample Synthesis, jointly optimizing these tasks in an end-to-end manner. By convolving synthesized one-shot samples with estimated onsets, akin to a drum machine, we reconstruct the individual drum stems and train a Deep Neural Network on the reconstruction of the mixture. Experiments on the StemGMD dataset demonstrate that IDM achieves separation quality comparable to state-of-the-art supervised methods that require isolated stems data.

**Index Terms**—audio source separation, deep learning, signal processing, analysis-by-synthesis

IN Western popular music, the rhythmic foundation typically relies on percussion instruments from a standard drum kit comprising kick drum, snare drum, and hi-hat, while additional elements such as cymbals, tom-toms, and auxiliary percussions provide timbral complexity and rhythmic variation. Music producers and engineers often need to adjust individual drum instruments separately for remixing, rebalancing, effects processing, or creating educational materials [1], [2]. Ideally, music production would use isolated recordings of each drum instrument (known as "stems"), allowing for precise control during mixing. However, these instruments are usually played simultaneously and by the same performer, resulting in recordings in which all elements are mixed into a single audio stream. Obtaining these separated stems during recording requires multiple microphones (leading to microphone bleeding) or asking musicians to play in unnatural conditions [3]. The need for tools that can extract individual drum stems from already mixed recordings has led to growing interest in Drum Source Separation (DSS) [4]–[6].

In the professional music production industry, commercial tools such as DrumsSSX<sup>1</sup> and Fadr<sup>2</sup> offer drum stem separation capabilities. These solutions, however, are proprietary and still have limitations in separation quality and flexibility.

DSS is challenging due to the acoustic properties of percussion sounds. Many percussive sounds lack a clear harmonic structure and exhibit broad spectral characteristics that typically overlap in both time and frequency domains. Additionally, there exists a wide diversity of percussive instruments, classified roughly into membranophones (e.g., kick drum, snare drum, toms) and idiophones (e.g., cymbals, hi-hats)

B. Torres, G. Peeters, and G. Richard are with the Laboratoire de Traitement et Communication de l'Information (LTCI), Télécom Paris, Institut Polytechnique de Paris, 91120 Palaiseau, France.

<sup>1</sup><https://fuseaudiolabs.de/#/pages/product?id=300867907>

<sup>2</sup><https://fadr.com/drum-stems>

[7]. While "drum", more strictly defined, refers to membranophones, we follow common usage for simplicity and use the term broadly to encompass all percussive instruments in this work. Each instrument can produce several sounds depending on the playing technique, further complicating the separation task. In addition to these complexities, drum-related music information research has received relatively limited attention, possibly reflecting Western music's historical emphasis on melodic and harmonic elements rather than rhythmic foundations found in traditions such as Indian tabla playing or African percussion-centered music.

In a broader context, Music Source Separation (MSS) has gained significant attention due to the impressive performance of deep learning methods. These approaches have achieved state-of-the-art results by training Deep Neural Networks (DNNs) in a supervised manner using ground-truth separated stems [6], [8], [9]. However, MSS benchmarks typically focus on isolating just four classes: vocals, drums, bass, and other instruments, considering the drum section as a single stem.

Recent works have capitalized on multitrack synthetic datasets generated by drum machines and programming software [6], [10] for training DSS models. Simultaneously, the MSS literature has shown promising results from joint separation and transcription approaches [11]. Complementing these developments, data-driven analysis-by-synthesis methods (i.e., learning to decompose a signal by resynthesizing it from estimated parameters) have demonstrated advances in techniques that do not require ground-truth data [12]–[14].

In this work, we propose an analysis-by-synthesis, multitask approach to DSS. By modeling drum tracks as sequences of one-shot samples triggered at precise times, similar to a drum machine, we train a DNN to recover both the transcription and one-shot samples from the reconstruction of the mixture. DSS is then achieved via audio synthesis from the "inverted" drum machine. Due to the strong inductive bias in our approach, we can bypass the need for isolated stems during training while achieving results comparable to state-of-the-art methods. This trade-off is advantageous, as datasets with transcription annotations are generally more accessible than those with clean, isolated multitrack recordings.

Conceptually, our approach is similar of drum replacement in music production, where drum tracks undergo manual onset detection and are replaced with one-shot samples from a sample library. We propose instead to perform this process in an automated, data-driven manner while learning to synthesize the actual one-shot samples from the mixture.

Our method, IDM, combines approaches from Automatic Drum Transcription (ADT), unsupervised source separation, and drum synthesis literature [13]–[16] to tackle DSS without

requiring separated stems, only requiring transcription annotations at training time. An open-source implementation of our method is available online<sup>3</sup>. Our main contributions are:

- A novel analysis-by-synthesis framework for Drum Source Separation (DSS) that works without isolated stems, relying only on transcription data for training.
- A jointly trained model that unifies Automatic Drum Transcription (ADT) and One-shot drum Sample Synthesis (OSS) in a single end-to-end system.
- A modular separation model that achieves separation quality comparable to supervised, state-of-the-art methods while using  $\approx 100$  times fewer parameters.

The remainder of this paper is structured as follows: Section I reviews related work in ADT, OSS, DSS, and analysis-by-synthesis. The proposed Inverse Drum Machine (IDM) is explained in Section II, and its experimental evaluation is detailed in Section III. We present and discuss the results in Sections IV and V and conclude in Section VI.

## I. RELATED WORK

This section presents relevant prior research in four interconnected areas that form the foundation of our approach: Automatic Drum Transcription (ADT), One-shot drum Sample Synthesis (OSS), Drum Source Separation (DSS), and Data-driven analysis-by-synthesis.

### A. Automatic Drum Transcription (ADT)

ADT aims to detect and classify percussion events within audio recordings, producing a symbolic representation (typically onset times and instrument classes) of the drum performance [17]. While ADT encompasses various formulations, this work focuses on Drum Transcription of Drum-only recordings (DTD), where the input consists exclusively of percussion instruments without melodic content.

Approaches to DTD have evolved from traditional signal processing methods to machine learning techniques. Non-negative Matrix Factorization (NMF) and its variants have seen considerable success [18] modeling spectral patterns of drum sounds without requiring labeled training data. More recent methods leverage deep learning, with both supervised [19], [20] and unsupervised [13] approaches showing significant performance improvements. Most DTD research has focused on a limited set of drum instruments, typically kick drum, snare drum, and hi-hat [2], [18], while some recent works have expanded the instrument vocabulary [13], [20]–[23].

### B. One-shot Drum Sample Synthesis

Percussion instruments typically produce sounds with broad spectral characteristics and exponentially decaying modes [24]. Drum sound synthesis has a rich history in commercial music production and academic research. Traditional approaches include physical modeling [24], [25], which simulates the acoustic properties of percussion instruments; spectral

modeling [26], [27], which represents sounds as sinusoids, filtered noise, and a transient component; and sample-based synthesis, which triggers pre-recorded audio samples.

Recent advances in generative deep learning have tackled drum sound synthesis research from a data-driven perspective, using convolutional neural networks [28] and generative adversarial networks [29]–[31]. Other techniques employ diffusion models [32] and Differentiable Digital Signal Processing (DDSP) [16], [33]. With particular relevance to this work, Shier et al. [16] proposed pairing a DDSP sinusoidal plus noise synthesizer with a transient enhancing Temporal Convolutional Network (TCN) to generate drum sounds. TCNs apply dilated convolutions to sequence data. This combination allows them to capture long-term dependencies with a large receptive field, making them effective for audio synthesis.

### C. Drum Source Separation (DSS)

Traditional DSS approaches have primarily relied on NMF-based methods, which model drum events as spectral templates repeatedly triggered over time [4]. These approaches decompose a spectrogram into a product of template and activation matrices, representing the spectral characteristics of different drum sounds and their temporal occurrences, respectively.

Conceptually, our approach shares several similarities with works based on Non-negative Matrix Factor Deconvolution (NMFD) [34] which incorporate transcription information into the initialization process [2], [5]. However, our method differs in several crucial aspects: (1) we operate directly in the time domain, providing immediate access to one-shot samples without requiring magnitude spectrogram inversion; (2) unlike NMFD, which performs per-track optimization on test-time, our approach incorporates a dedicated training stage that optimizes neural network parameters through gradient descent; (3) our method can bypass Wiener filtering (which typically uses the phase from the mixture) to obtain separated sources.

In DSS literature, NMFD methods have also been used in a cascaded manner [5] to reduce cross-talk between instruments, and tested for dual-channel input [35]. Vande Veire et al. [15] introduced Sigmoidal NMFD, which enforces impulse-like behavior in the updated activations by factoring them into an onset and an amplitude component, and updating them using gradient descent.

Despite their effectiveness in controlled settings, NMFD-based methods have limited flexibility since they operate at test time and are typically trained on a per-track basis. Moreover, while these approaches have demonstrated reasonable performance on datasets with few instrument classes, they have not been extensively evaluated on large-scale datasets with numerous percussion types.

A significant advancement in DSS came with the development of the StemGMD dataset [6], which leveraged MIDI transcriptions from the GMD dataset [36], captured from performances on an electronic drum kit, to synthesize individual drum stems for nine drum classes. With it, the first deep neural network specifically designed for drum source separation was introduced, capable of separating five stems from a stereo drum mixture: kick drum, snare drum, toms, hi-hat, and cymbals. A recent benchmark of deep MSS

<sup>3</sup><https://github.com/bernardo-torres/inverse-drum-machine>

architectures trained on StemGMD [10] shows that there is room for improvement by using larger, more complex models, in particular those that are trained to perform waveform synthesis directly (rather than relying on time-frequency masking). Unlike NMFD, these DNN models require supervised training with ground-truth separated stems and often have a high parameter count, making them computationally expensive and data-intensive.

#### D. Data-driven Analysis by Synthesis

A growing body of research combines data-driven methods with analysis-by-synthesis approaches. Differentiable Digital Signal Processing (DDSP) combines gradient descent (particularly in automatic differentiation frameworks) with Digital Signal Processing (DSP) [37], enabling end-to-end training of models that incorporate signal processing operations within their architectures. This paradigm has been applied in several works for the estimation of synthesizer parameters [16], [25], [38]–[40].

A typical scenario is training DNNs to predict DSP parameters for synthesis by comparing reconstructed audio to a target. Spectral loss functions, such as multi-resolution Short-Time Fourier Transform (STFT) loss, are commonly used instead of waveform loss to avoid phase alignment issues.

In source separation, analysis-by-synthesis has been employed to estimate the parameters of musical sources from mixture inputs. These parameters drive source models to resynthesize individual sources that are summed and compared to the original mixture [14], [41]. This approach has proven particularly effective for separating singing voices in choir ensembles [14], [42], where multi-pitch information guides the separation process.

In the context of ADT, reconstruction of drum tracks has been used for evaluating transcription performance through listening tests [20]. For unsupervised ADT, Choi and Cho [13] resynthesize tracks from estimated transcriptions using randomly selected one-shot samples from a class-sorted collection, training a DNN using an onset-enhanced reconstruction loss. Our work extends their method to DSS.

## II. METHOD

In this work, we propose an analysis-by-synthesis approach to decompose drum mixtures into transcription information and elementary one-shot samples. As illustrated in Figure 1, the proposed architecture processes audio mixtures through several stages. Initially, a Feature Extraction module derives frame-level representations from the input mixture. These features are subsequently transformed by a Synthesis Conditioning module into relevant parameters for synthesis (transcription and one-shot conditioning). The conditioning is used by a one-shot synth to synthesize drum samples which are sequenced by the estimated transcription. A multitask objective enables all modules to be trained jointly, using ground-truth transcriptions as supervision. At inference time, the model operates on the audio mixture alone; however, its modular design allows users to optionally provide external information, such as a corrected transcription.

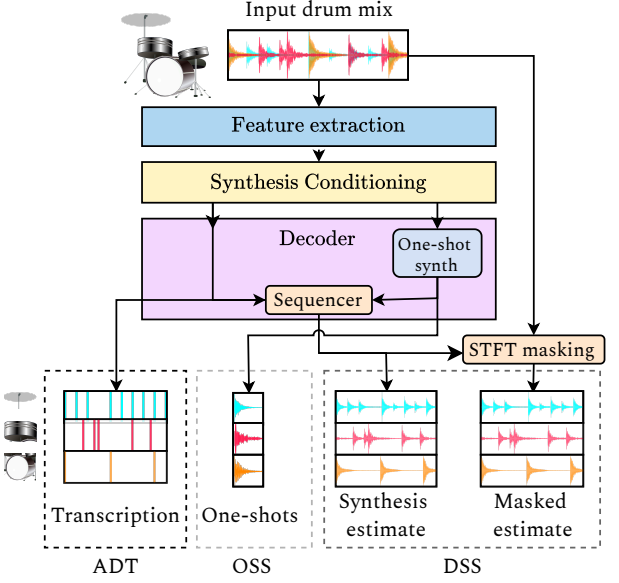


Fig. 1. The proposed separation model processes the audio input through several stages. First, a Feature Extraction module extracts learned frame-level features. These features are transformed by a Synthesis Conditioning module into relevant synthesis parameters: transcription onsets, velocities, a mixture embedding, and individual track gains. A decoder module synthesizes one-shot samples for each drum instrument conditioned on the mixture embedding and reconstructs individual drum tracks by sequencing these one-shots with the obtained transcription. The framework encompasses three interconnected tasks: Automatic Drum Transcription (ADT), One-shot drum Sample Synthesis (OSS), and Drum Source Separation (DSS). DSS is obtained either from the decoder output (*synthesis estimate*) or after time-frequency masking (*masked estimate*).

The following sections explain the proposed multitask framework and then go into detail on the Feature Extraction, Synthesis Conditioning, and Decoder modules, which are also detailed in Figure 2. For presentation clarity, we leave most implementation details to Section II-F.

#### A. Multitask learning for Drum Source Separation

Our approach encompasses three interconnected tasks:

- 1) **Automatic Drum Transcription (ADT):** The precise estimation of the onset times of each drum instrument is achieved by training a transcription head to predict onset activations.
- 2) **One-shot drum Sample Synthesis (OSS):** High-quality one-shot samples for each drum instrument are generated by a TCN conditioned on instrument type and mixture embedding.
- 3) **Drum Source Separation (DSS):** Individual drum tracks are extracted from the mixture by sequencing the synthesized one-shot samples with the estimated transcription.

To train our analysis-synthesis framework we analyze an input mixture  $x$  and recompose the individual drum tracks by sequencing onset activations with generated one-shot samples. Individual tracks are mixed together to obtain a reconstructed mixture  $\hat{x}_{\text{synth}}$ . The entire framework is trained end-to-end with a reconstruction loss  $\mathcal{L}_{\text{recon}}$ , with the addition of a transcription loss  $\mathcal{L}_{\text{trans}}$  and a mixture embedding loss  $\mathcal{L}_{\text{emb}}$ . Sections III-B and III-C provide details on the training step and objective.

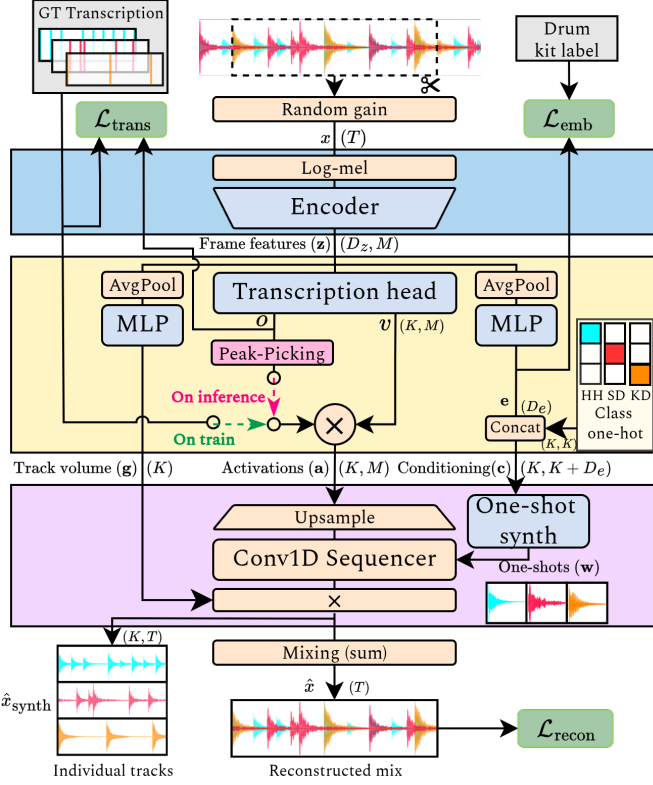


Fig. 2. Detailed diagram of the analysis-by-synthesis pipeline, containing the Feature Extraction (blue), Synthesis Conditioning (yellow), and Decoder (purple) modules. Blocks in blue indicate trainable components, blocks in orange indicate differentiable operations, and blocks in pink indicate non-differentiable operations. Loss functions are represented as green components, and grey components represent external information used during training

### B. Feature Extraction

Our Feature Extraction module learns features  $\mathbf{z}$  which contain relevant information for the transcription and mixture embedding. It begins by computing Log-Mel Spectrograms from the input waveform  $\mathbf{x}$  at  $f_s = 44.1$  kHz. Then, a ConvNeXt encoder [43] (Section II-F2) processes the spectrogram to extract frame-level representations  $\mathbf{z} \in \mathbb{R}^{D_z \times M}$ , where  $D_z = 32$  denotes the dimension of the frame features and  $M$  represents the number of spectrogram frames.

### C. Synthesis Conditioning

The Synthesis Conditioning module transforms the frame features into parameters that guide the reconstruction process: transcription onsets, velocities, individual track gains, and a conditioning vector. Estimated onsets and velocities are multiplied and upsampled to obtain an activation signal used to trigger one-shot samples, composing the individual tracks for  $K$  predefined drum classes. The conditioning vector is used as conditioning for the one-shot synthesis model, guiding the generation of one-shot samples based on the instrument class and a mixture embedding, which controls the timbral variations within a given class.

1) **Transcription head:** The transcription head (Section II-F3) transforms features  $\mathbf{z}$  into a factorized representation of the drum component activation signal, composed of:

(i) an onset signal  $\mathbf{o} \in [0, 1]^{K \times M}$ , identifying when each instrument is played; and (ii) a velocity signal  $\mathbf{v} \in [0, 2]^{K \times M}$ , capturing the intensity of each onset. This architecture draws inspiration from the "Onsets and Frames" [20], [44] and Sigmoidal NMFD [15] papers. We use the name velocity as a reference to *MIDI velocity*, a control signal used to represent note intensity. However, we only use  $\mathbf{v}$  to represent the one-shot volume and it does not affect timbre. The temporal resolution is set by the spectrogram's hop size.

2) **Activation signal:** We compose  $\mathbf{a}^{(T)} \in \mathbb{R}^{K \times T}$ , the activation signal, by stacking the individual instrument activations  $\mathbf{a}_k$ , which are derived by element-wise multiplication of onsets and velocities, followed by upsampling from the rate of the frames  $m$  to the rate of the signal time  $t$ :

$$\mathbf{a}_k^{(T)} = \text{upsample}(\mathbf{o}_k \odot \mathbf{v}_k) \quad (1)$$

We upsample using zero insertion [13]. While this approach induces aliasing, we found that if the onset signal is sparse enough, the synthesis artifacts are negligible. We therefore separate training and inference behavior to minimize these effects during training.

During **training**, we pass ground-truth onsets instead of  $\mathbf{o}$  to compose the activation signal  $\mathbf{a}$ . Note that the onset signal is still used for training the transcription head from the transcription loss, but we effectively stop the gradient flowing from the reconstruction process to  $\mathbf{o}$ . The gradient passed to the velocity branch, however, remains intact. During **inference**, we apply peak picking (Section II-F4) to extract sparse onsets from  $\mathbf{o}$ .

3) **Mixture embedding:** To represent the overall timbral characteristics of the drum-kits (not of the specific instruments), we derive a mixture embedding  $\mathbf{e} \in \mathbb{R}^{D_e}$  from frame features  $\mathbf{z}$  using a Multi-Layer Perceptron (MLP) (please refer to Section II-F5 for architectural details). An ideal conditioning embedding should be capable of summarizing the timbre of an instrument as well as acoustic conditions while learned without supervision. As a simpler method given the small number of drum kits used in our experiments we learn mixture embeddings by matching one-hot labels constructed from drum kit annotations using a classification loss  $\mathcal{L}_{emb}$  (Section III-C). This branch behaves as a "drum kit classifier" and restricts the model to synthesize only from drum kits observed during training, but serves as proof-of-concept for a disentangled class/timbre conditioning mechanism.

4) **Track volume:** We estimate global track gains  $\mathbf{g} \in [0, 2]^K$  from  $\mathbf{z}$  using a MLP (Section II-F5).

5) **Conditioning vector:** Recall that  $K$  is the number of drum instruments. A class conditioning vector  $\mathbf{c}$  is composed by broadcasting  $\mathbf{e}$  to  $(K, D_e)$  and concatenating ( $\oplus$ ) the  $K$ -dimensional one-hot encodings of the different classes in the feature dimension, resulting in size  $(K, K + D_e)$ .  $\mathbf{c}$  can be interpreted as the stack of individual class/mixture conditioning vectors for all classes of a particular mixture ( $\{\mathbf{c}_k\}_{k=1}^K$ , where  $\mathbf{c}_k = \mathbf{e} \oplus \text{one-hot}(k)$ ).

### D. Decoder

The Decoder module synthesizes one-shot samples for each drum instrument and reconstructs individual drum tracks by

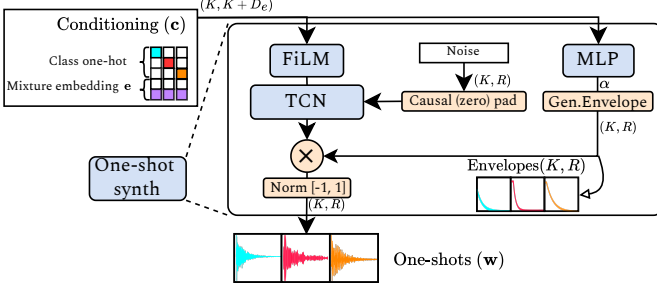


Fig. 3. One-shot synth model architecture. White noise is fed to a Temporal Convolutional Network (TCN) conditioned via Feature-wise Linear Modulation (FiLM) on a conditioning vector  $\mathbf{c}$ , which has disentangled instrument class/timbre dimensions. Causal zero padding is applied. The output is shaped by a parametrized exponential envelope estimated from  $\mathbf{c}$  and normalized to  $[-1, 1]$  amplitude range.  $\mathbf{c}$  controls the drum kit (mixture embedding) and drum instrument (class one-hot) synthesized by the TCN.

sequencing these one-shots with the activations from the Synthesis Conditioning module. The decoder is composed of two main components: a one-shot synth and a sequencer.

1) **One-shot Synth:** Conditional One-shot drum Sample Synthesis is performed with a Temporal Convolutional Network (TCN), similar to the work of Shier et al. [16]. However, instead of using TCN to enhance the transient of a sinusoidal-plus-noise signal [27], we take a more direct path. We eliminate the sinusoidal-plus-noise input, instead feeding white noise directly to the TCN. By expanding the network's receptive field and adding a time envelope, we found the TCN capable of synthesizing both sinusoidal, noise, and transient components. Importantly, in order to assure the TCN output has length of 1 second, the input white noise is left zero-padded accordingly. This causal padding is also essential for modeling the transient. By providing a block of zeros before the noise, we encourage the TCN to not operate in a continuous steady-state mode during the transient period. Figure 3 shows the architecture of the one-shot synthesis model, with specific implementation details reported in Sections II-F6 to II-F8.

To guide the synthesis process, we follow [16] and condition the TCN using FiLM [45] on a conditioning vector  $\mathbf{c}$  composed of two disentangled dimensions: a mixture embedding  $\mathbf{e}$  and the instrument class one-hot encoding. To model the natural energy decay typical of percussion instruments, an exponential amplitude envelope is multiplied to the TCN output, controlled by a decay parameter  $\alpha$  dependent on  $\mathbf{c}$ .

Unlike most OSS approaches [16], [30], [32], we train the synthesizer model on mixture track reconstructions rather than isolated one-shot samples, making it inherently reliant on accurate onset placement.

2) **Sequencer:** The sequencer serves as the bridge between transcription and synthesis, transforming drum instrument activations and one-shot samples into full individual tracks. Let  $\mathbf{w} \in [-1, 1]^{K \times R}$  represent a set of time-domain one-shot signals (one second in duration). The reconstructed mixture  $\hat{\mathbf{x}}_{\text{synth}} \in \mathbb{R}^T$  is obtained by:

$$\hat{\mathbf{x}}_{\text{synth}} = \sum_{k=1}^K \mathbf{g}_k \text{Sequencer}(\mathbf{w}_k, \mathbf{a}_k^{(T)}) \quad (2)$$

The sequencer is implemented as a convolutional operator using frequency domain multiplication [13].

### E. Time-frequency masking

Although separated sources can be directly obtained by synthesis, previous work showed that improved results can be obtained after using them for spectral masking of the mixture [14]. In this work, we employ  $\alpha$ -Wiener Masking [46] (during inference only), which uses our synthesized individual tracks to create Time-Frequency (TF) masks applied to the original mixture. The underlying principle is that each stem's spectrogram contributes proportionally to the energy in each TF bin of the mixture's spectrogram (see Section II-F9 for details).

### F. Implementation details

1) **Log Mel Spectrogram:** We compute Log Mel Spectrograms with 128 mel frequency bands, a window size of 2048 samples, and a hop size of 512 samples (11.6ms), corresponding to 86.1 Hz activation rate.

2) **Encoder Architecture:** Our ConvNeXt encoder begins with a transition convolutional layer downsampling the feature dimension by 4, followed by LayerNorm [47]. Four hierarchical stages follow with feature dimensions  $[4, 8, 16, D_z]$ , each starting with a channel downsampling block (LayerNorm +  $3 \times 3$  convolution). Each stage contains multiple residual blocks with  $7 \times 7$  depthwise separable convolutions, LayerNorm, GELU activations, and pointwise transformations. Unlike the original ConvNeXt, we maintain temporal resolution between stages. As demonstrated in [22], the specifics of the architecture might not have a big impact on ADT performance. We thus opted for a modern, well-validated off-the-shelf convolutional architecture.

3) **Transcription Head:** The frame features  $\mathbf{z}$  are processed through a 1D convolutional layer with ReLU activation, followed by parallel onset and velocity branches with linear layers. The onset branch outputs sigmoid activations, while the velocity branch uses exponentiated sigmoid activation [37]. We did not include a sequence model as we found it unnecessary for achieving reasonable transcription performance.

4) **Peak Picking:** We apply peak picking to the frame-rate onset signal during inference to extract sparse onsets and remove low amplitude activations. We follow the heuristic and hyperparameters from [13], [48].

5) **Mixture Embedding and Track gain MLPs:** Both MLP architectures first remove the time dimension from the frame features  $\mathbf{z}$  via temporal average pooling. The Mixture Embedding MLP then applies a LayerNorm layer, followed by a two-layer ReLU network that maps dimensions from  $D_z \rightarrow D_z \rightarrow D_e$ . For the track gains, a separate three-layer MLP with LeakyReLU activations is applied per instrument, with layer dimensions mapping from  $64 \rightarrow 16 \rightarrow 16 \rightarrow 1$ .

The final layer uses an exponentiated sigmoid activation [37] to estimate each gain parameter  $g_k$ .

6) **TCN Architecture:** Our TCN [16] consists of 12 dilated causal convolutional layers with residual connections and GELU activations. Input is projected to a latent dimension of 48, processed through the dilated residual blocks (dilation doubling at each layer, starting from 1), and projected back to audio dimensions. The total receptive field is  $\approx 1.3s$ . Kernel size is 15 throughout, with instance normalization applied to all layers and output normalized to  $[-1, 1]$ .

7) **FiLM Conditioning:** Conditioning is implemented as a stack of linear layers mapping from  $\mathbf{c}$  to shift/scale parameters applied after the GELU activation in each TCN layer:

$$\text{FiLM}(\mathbf{x}_{ij}, \mathbf{c}) = \gamma_{ij}(\mathbf{c}) \cdot \mathbf{x}_{ij} + \beta_{ij}(\mathbf{c}), \quad (3)$$

where  $\mathbf{x}_{ij}$  is the  $j$ th feature map of the  $i$ th TCN layer (after GELU),  $\mathbf{c}$  is the conditioning vector, and  $\gamma_{ij}(\mathbf{c})$  and  $\beta_{ij}(\mathbf{c})$  are the shift and scale parameters learned by the  $(i, j)$ th linear layer.

8) **Envelope:** A 2 layer MLP with ReLU activation and exponentiated sigmoid estimates envelope parameter  $\alpha$  from the conditioning vector. The envelope is applied to the TCN output by element-wise multiplication:

$$\text{Gen. envelope}(\alpha) = e^{-20 \cdot \alpha \cdot \frac{t}{R}} \quad \text{for } t \in \mathbb{Z}, 0 \leq t < R \quad (4)$$

9) **TF Masking:** Given a mixture complex STFT  $\mathbf{X}$  and an estimated source STFT  $\hat{\mathbf{X}}_{\text{synth},i}$ , time-frequency masks  $\mathbf{M}_i$  and masked spectrograms  $\hat{\mathbf{X}}_{\text{mask},i}$  are computed as:

$$\mathbf{M}_i = |\hat{\mathbf{X}}_i|^\alpha \oslash \left( \sum_j |\hat{\mathbf{X}}_j|^\alpha + \epsilon \right) \quad \text{and} \quad \hat{\mathbf{X}}_{\text{mask},i} = \mathbf{M}_i \odot \mathbf{X}, \quad (5)$$

where  $\odot$  and  $\oslash$  denote element-wise multiplication and division, respectively, and  $\epsilon$  is a small constant to prevent division by zero. We denote  $\hat{x}_{\text{mask}}$  the waveform estimates obtained after inverse STFT of  $\hat{\mathbf{X}}_{\text{mask},i}$  using the mixture phase.  $\alpha$  is set to 1 in order to remain consistent with [5], [6].

### III. EXPERIMENTS

This section describes our experimental methodology for training and testing the proposed drum source separation framework. Our primary experimental configuration uses a drums-only database with ground-truth transcription annotations and separated stems as a test-set. The following subsections detail the data, experimental protocols, hyperparameters, and baseline methods employed in our work.

#### A. Datasets

Our experiments are conducted using the StemGMD dataset [6], which builds upon the MIDI data from the GMD dataset [36] by synthesizing isolated drum stems for 9 canonical instruments across 10 distinct drum kits. StemGMD has approximately 136 hours of mixture data. Perfect transcription annotations were extracted directly from the associated MIDI files. Table I presents the mapping between the original instrument nomenclature, the names used in the audio files

TABLE I  
DRUM CLASS CONFIGURATIONS. INSTRUMENT NAMES CORRESPOND TO COMMON DRUM KIT TERMINOLOGY, WHILE 9-CLASS AND 5-CLASS REFER TO THE GROUPINGS USED IN OUR EXPERIMENTS. 9-CLASS NAMING IS CONSISTENT WITH THE STEMGMD DATASET. OUR MODEL IS TRAINED ON THE 9-CLASS CONFIGURATION AND IS ABLE TO SEPARATE AN INPUT MIXTURE INTO 9 DRUM CLASSES. THE 5-CLASS CONFIGURATION, USED FOR EVALUATION ONLY, GROUPS SIMILAR INSTRUMENTS TOGETHER.

Instrument Name	9-Class (train/test)	5-Class (test)
Kick Drum	kick	Kick (KD)
Snare Drum	snare	Snare (SD)
Closed Hi-Hat	hihat_closed	
Open Hi-Hat	hihat_open	Hi-Hats (HH)
High-Mid Tom	hi_tom	
Low Tom	mid_tom	Toms (TT)
High Tom	low_tom	
Crash	crash_left	
Ride	ride	Cymbals (CY)

(9-Class), and the two instrument groupings employed in our experimental design. Training uses the 9-Class configuration, while evaluation is performed on both 9-Class and 5-Class groupings. To maintain comparability with baseline LarsNet (Section III-D), which withheld 4 kits during training, we use only 6 of the 10 drum kits available in the dataset ( $D_e = 6$ ).

We follow the provided train, validation, and test splits on the MIDI track level. Contrary to LarsNet [6], which uses a small subset of the test partition named *eval session*, we evaluate our models on the entire test split, which comprises  $\sim 10$  h of mixture data. We found that the *eval session* removed substantially the toms and cymbals from the test set, and by increasing its size we achieve a more balanced evaluation.

#### B. Training

Our training protocol uses randomly cropped audio segments of  $T = 6$  seconds at sampling rate  $f_s = 44.1$  kHz, normalized to the amplitude range  $[-1, 1]$ . Cropped tracks are resampled and converted to mono on-the-fly. We apply random gain augmentation to obtain input  $\mathbf{x}$ , with gain values sampled from a uniform distribution in the range  $[0.3, 1.0]$  with a probability of 0.8. We use no additional data augmentations.

Transcription activations and a conditioning vector ( $\mathbf{c}$ ) are extracted from  $\mathbf{x}$ . Then, individual one-shot samples ( $\mathbf{w}$ ) for each drum instrument are synthesized from  $\mathbf{c}$  and sequenced into full tracks using the activations. The individual tracks are mixed to obtain a reconstructed mixture  $\hat{\mathbf{x}}$ , and reconstruction loss  $\mathcal{L}_{\text{recon}}$  is applied between  $\hat{\mathbf{x}}$  and  $\mathbf{x}$ . The entire framework is trained end-to-end, with the addition of a transcription loss  $\mathcal{L}_{\text{trans}}$  and a mixture embedding loss  $\mathcal{L}_{\text{emb}}$  (Section III-C).

For the training phase, we configure the number of drum instruments as  $K = 9$ , enabling separation of the input mixtures into 9 distinct drum classes (as enumerated in Table I). Training consists of 800 epochs with a batch size of 33, using the Adam optimizer with a learning rate of  $5 \times 10^{-3}$  and gradient clipping with a threshold value of 0.5. We implement

TABLE II  
COMPARISON OF DIFFERENT METHODS FOR DRUM SOURCE SEPARATION,  
BASELINES AND PROPOSED MODEL. TRANSC. = TRANSCRIPTION.

Method	External information used		Input for eval. (kHz/channels)
	Training	Inference	
Oracle	–	Isolated stems	44.1/mono
NMF 1A	–	Transc. + one-shots	44.1/mono
NMF 1B	–	Transc. + one-shots	44.1/mono
NMF 3	–	Transc.	44.1/mono
LarsNet	Isolated stems	–	44.1/stereo
LarsNet Mono	Isolated stems	–	44.1/mono
IDM (ours)	Transc.	–	44.1/mono
IDM+ onsets	Transc.	Transc.	44.1/mono

model checkpointing based on the mean validation loss  $\mathcal{L}_{\text{total}}$  across tracks (no cropping is performed on the validation data). We keep only the shortest 550 validation tracks for a more efficient validation. Our total parameter count is of 542.1K.

### C. Training Objective

The system is trained end-to-end using a combination of reconstruction, transcription, and mix embedding losses. The reconstruction loss  $\mathcal{L}_{\text{recon}}$  is computed between the synthesized mixture and the input cropped mixture. We set  $\mathcal{L}_{\text{recon}}$  to be the Multi-Resolution STFT Loss [37], [49]:

$$\mathcal{L}_{\text{recon}}(\mathbf{x}, \hat{\mathbf{x}}_{\text{synth}}) = \sum_{\gamma \in \Gamma} \left\| |\mathbf{X}^{(\gamma)}| - |\hat{\mathbf{X}}^{(\gamma)}| \right\|_1 + \left\| \log(|\mathbf{X}^{(\gamma)}|) - \log(|\hat{\mathbf{X}}^{(\gamma)}|) \right\|_1, \quad (6)$$

where  $(\mathbf{x}, \hat{\mathbf{x}}_{\text{synth}})$  are the time domain input and the reconstructed signals and  $\mathbf{X}^{(\gamma)} = \text{STFT}^{(\gamma)}(\mathbf{x})$  is the STFT of  $\mathbf{x}$  at scale  $\gamma$ . The set of scales  $\Gamma$ , expressed in number of samples of the analysis window, is set to [2048, 1024, 512, 256], and the hop sizes are set to a quarter of the analysis window size.

Transcription loss  $\mathcal{L}_{\text{trans}}$  is the Binary Cross-Entropy loss between the estimated onsets and the ground-truth onsets for all drum instruments. Since ground-truth annotations are available as a list of onset times, in order to obtain onset target signals for training, we create a sequence containing  $M$  zeros (in the same rate as the activation rate) and set frames closest to the annotation time to 1. The mixture embedding loss  $\mathcal{L}_{\text{emb}}$  is essentially a drum kit classification loss, implemented as the Cross-Entropy between the estimated mixture embedding  $\mathbf{e}$  and the one-hot drum kit label. The training objective is the sum of the three losses:

$$\mathcal{L}_{\text{total}} = \mathcal{L}_{\text{recon}} + \mathcal{L}_{\text{trans}} + \mathcal{L}_{\text{emb}} \quad (7)$$

### D. Baselines

We evaluate our approach against both learning-free<sup>4</sup> baselines and a deep supervised baseline. Table II summarizes our

experimental comparison and the varying levels of external information used during training and inference phases.

1) **Learning-free**: The learning-free baseline methodology was proposed in [2], [5]. This approach is based on NMF [34], wherein the mixture's spectral magnitude is modeled as the product of template and activation matrices. Their work employs informed NMF variants where drum transcription information and spectral templates from drum one-shots are used for NMF algorithm initialization. We replicate experimental cases 1A, 1B, and 3 from their work for direct comparison with our method. In all three cases, the activation matrix is initialized with ground-truth transcription information with values of 1 where onsets occur and a small constant  $\epsilon = 10^{-10}$  elsewhere.

Following [6], we use a StemGMD partition containing isolated one-shots synthesized with identical drum kits for template initialization for 1A and 1B (*single hits* partition). In case 3, spectral templates are initialized with random values. Both 1A and 1B use transcription and template initialization, but in 1A, spectral templates remain fixed while only the activation matrix is updated. We denote these baselines by NMF 1A, NMF 1B, and NMF 3, respectively.

We adapted the STFT parameters to accommodate our 44.1 kHz sample rate while maintaining time resolution and window size consistency with the original implementation. In contrast to findings reported in [6], we observed a drop in performance when increasing the number of iterations. Consequently, we conducted a grid search on the validation set, varying template length and iteration count for each case. Our hyperparameter search determined that 50 iterations resulted in optimal performance for the case with fixed templates (NMF 1A), while 20 iterations (NMF updates) were best for NMF 1B and NMF 3. For the template length, we found that 40, 10, and 7 yielded the best results respectively. We increased  $\epsilon$  to  $10^{-10}$  to address convergence issues observed with smaller values. The number of templates was configured to match the number of drum instruments (9). All other implementation details were preserved as specified in the original publication. NMF baselines were reimplemented using TorchNMF<sup>5</sup> following an open source reference code [50].

2) **Supervised DNN**: We benchmark our method against the deep learning model LarsNet, which was trained for drum separation in a fully supervised manner using isolated stems [6] and its available open source<sup>6</sup>. LarsNet was trained on StemGMD multitrack data, using 6 of the 10 available drum kits. The model has 49.1M parameters, operates at 44.1 kHz, and was trained on stereo files to separate stems in the 5-Class configuration. To ensure a fair comparison, we provide the model with 44.1 kHz stereo inputs to obtain stereo separated estimates, then convert them to mono. When evaluated in the *masking* configuration, we use these estimates to compute  $\alpha$ -Wiener masks and apply them to the mixture spectrogram. We also report metrics when removing spatial information from the input (LarsNet Mono) by averaging the stereo channels and duplicating the mono input.

<sup>4</sup>We consider a method learning-free if it does not have a data-driven training stage designed to generalize to unseen data at test-time.

<sup>5</sup><https://github.com/yojolicoris/pytorch-NMF>

<sup>6</sup><https://github.com/polimi-ispl/larsnet>

3) **Onsets on inference time:** Due to our modular synthesis approach, we can override the class onset predictions  $o_k[m]$  during inference with the ground-truth (while keeping velocities  $v_k[m]$ ). This provides an upper performance bound by isolating transcription limitations from synthesis capabilities. This approach offers insights into the separation performance with perfect onset detection. We add `+ onsets` to the model name when reporting these results.

### E. Evaluation

We implement a comprehensive evaluation framework combining transcription and separation metrics. It is noteworthy that the DSS task encompasses multiple drum classes with predominantly sparse activations (such as tom-toms), requiring careful consideration in the evaluation protocol. All metrics are computed per class, using full tracks as input, and aggregated across tracks. For all metrics except Predicted Energy in Silence (PES), evaluation is restricted to active stems, defined as stems containing at least one onset during the track duration. This methodological decision results in variable sample sizes (number of tracks) for the different classes. The "Overall" metrics reported are computed as the aggregation of scores across all tracks, flattened and independent of class. We found this methodology to best represent the actual class distribution in the dataset.

During evaluation, input mixtures are generated dynamically through summing constituent stems. For the 5-Class evaluation configuration, we sum the stems within the same instrument groups to establish the target stems (e.g., hihat\_closed and hihat\_open are combined into a single Hi-Hats stem). We also sum model outputs accordingly.

1) **Transcription:** We extract discrete onsets from the estimated onset signal through peak picking, following the methodology detailed in Section II-F4. Precision and recall metrics are then computed for each drum class using the `mir_eval` python package [51]. The precision metric quantifies the proportion of detected onsets that correspond to actual events, while recall measures the proportion of actual events that are successfully detected by the system.

Transcription evaluation is performed exclusively on our model. We emphasize that our transcription performance assessment is not intended as a direct comparison with state-of-the-art drum transcription systems (which typically incorporate multiple datasets and extensive augmentation strategies), but rather as a measure of our system's intrinsic transcription capabilities and associated limitations. Moreover, even though DTD is considered a relatively simple task in ADT literature [17], [22], most works do not consider the full range of drum instruments present in our dataset.

2) **Source separation:** Our separation evaluation methodology is designed to assess both direct synthesis and masking-based separation capabilities. For each input mixture  $\mathbf{x}$ , the model generates synthesized estimates  $\hat{\mathbf{x}}_{\text{synth}}$  directly produced by our generative model.

We also compute masked estimates  $\hat{\mathbf{x}}_{\text{mask}}$  through time-frequency masking of the input mixture (Section II-F9). While masking techniques have been extensively employed in source

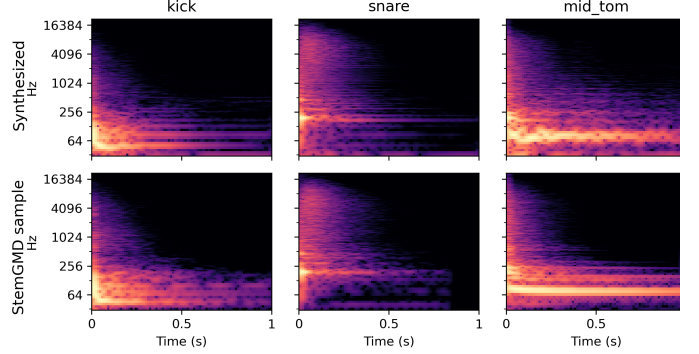


Fig. 4. Log-magnitude spectrograms of synthesized, one-second-long one-shot synthesized (top) and real (bottom) samples for three instruments. The real samples are taken from the StemGMD *single hits* partition with the second-highest velocity. Y axis is scaled in log frequency for better visibility, and warmer colors represent higher intensity.

separation literature, they exhibit known limitations including spectral leakage artifacts. Synthesis, conversely, provides a more direct assessment of the model's capacity to generate authentic drum sounds but may suffer from phase misalignment with the ground-truth. We therefore evaluate synthesis and masking outputs independently.

For each active stem, we compute both waveform and perceptual metrics between model outputs and ground-truth stems, with waveform metrics being the standard in source separation literature [9], [52].

To quantify separation quality in the waveform domain, we use the Signal to Noise Ratio, or Signal-to-Distortion Ratio (nSDR) as defined in [6], [9], computed exclusively for masked outputs ( $\hat{\mathbf{x}}_{\text{mask}}$ ):

$$\text{nSDR} = 10 \log_{10} \left( \frac{\|s\|^2}{\|s - \hat{s}\|^2 + \epsilon} \right), \quad (8)$$

where  $\epsilon = 10^{-8}$ . However, spectral similarity often correlates more strongly with human perceptual judgments than signal-based methods [53]. We therefore employ the Log Spectral Distance (LSD) as proxy for perceptual similarity:

$$\text{LSD}(s, \hat{s}) = \frac{1}{T} \sum_{t=1}^T \sqrt{\frac{1}{F} \sum_{f=1}^F \left( \log \frac{|\hat{\mathbf{S}}_{t,f}|^2 + \epsilon}{|\mathbf{S}_{t,f}|^2 + \epsilon} \right)^2} \quad (9)$$

where  $\mathbf{S} = \text{STFT}(s)$  with window length of 2048 and hop length of 512, and  $s$  and  $\hat{s}$  are the estimated and ground-truth signals.

Predicted Energy in Silence (PES) [54] is employed to quantify how accurately models predict silence when the corresponding ground-truth stem is silent (inactive). PES is defined as the average energy of estimated stems during silent ground-truth frames. The estimated and ground-truth signals are segmented using non-overlapping windows of size 512, retaining only frames corresponding to inactive ground-truth segments. Energy (in decibels) of estimated stems is computed as  $10 \times \log_{10}(\sum_n (x(n)^2) + 10^{-8})$ . We set our minimum threshold for silent frames to  $-60\text{dB}$ , clipping values below. PES is more relevant for synthesized outputs than for masked

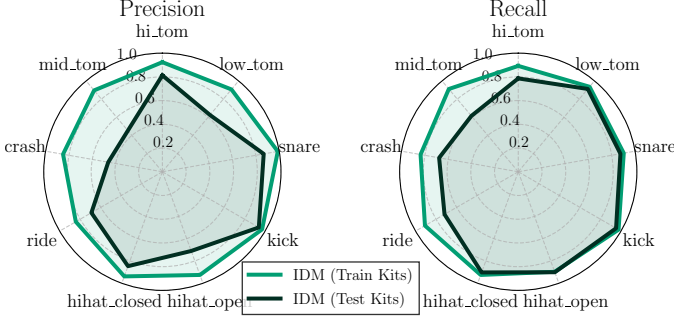


Fig. 5. Performance of the transcription module.

estimates, as we observed that TF masking introduce cross-talk artifacts that manifest as unwanted energy during silence.

For nSDR, higher is better, while for LSD and PES, lower is better.

#### IV. RESULTS

In this section, we present a comprehensive evaluation of our proposed Inverse Drum Machine (IDM) method and baselines, analyzing both transcription (Section IV-B) and separation (Section IV-C) performance. In addition to the objective metrics shown in this paper we have made available in an accompanying website<sup>7</sup> examples of the separated stems for all models discussed, along with the synthesized one-shot samples of our model.

For box plots, the central mark indicates the median of scores across tracks, the edges of the box are the 25th and 75th percentiles, and the whiskers extend to the full range of the data points.

##### A. One-Shot sample synthesis

Our model effectively learned to synthesize drum one-shots from 9 instruments across 6 drum kits. We provide a qualitative analysis of a few synthesized one-shots and refer the reader to the supplementary material for a full set of samples. Figure 4 shows examples of synthesized one-shots for a kick, snare and a tom-tom, with a reference one-shot taken from the StemGMD *single hits* partition (second highest velocity). The generated samples demonstrate the model’s ability to generate realistic drum sounds, capturing transient and steady-state components of each instrument.

##### B. Transcription Results

As shown in Figure 5, the trained transcription module achieves high precision and recall values (both in the 90s percentile range) across most instruments in the test tracks. This strong performance is partly due to the controlled experimental conditions, including low data diversity, as the degraded precision on the held-out kits shows.

The results reveal some variations across drum instruments. We observe particularly challenging detection patterns for cymbals, and toms. Despite these challenges, the overall transcription accuracy remains robust, providing a solid foundation for the subsequent separation task.

<sup>7</sup><https://bernardo-torres.github.io/projects/inverse-drum-machine/>

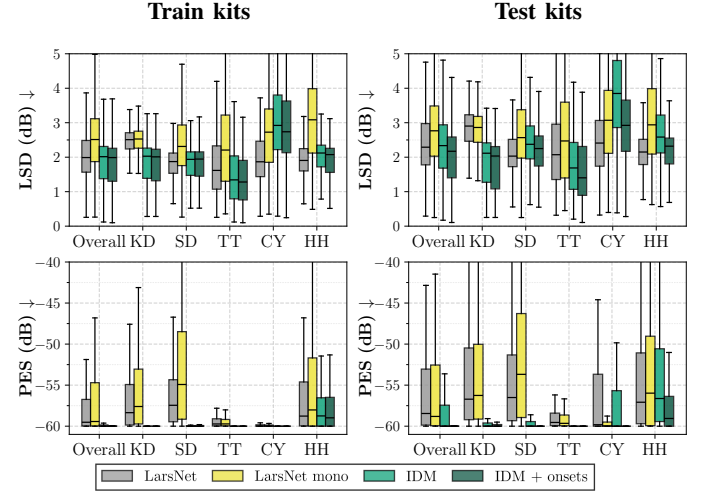


Fig. 6. Comparison of synthesis-based separation metrics. Top row shows Log Spectral Distance (LSD); bottom row shows Predicted Energy in Silence (lower is better for both). Left column is train kits; right is test kits.

##### C. Separation Results

1) **Direct synthesis results:** Figure 6 presents the synthesis-based separation results using Log Spectral Distance (LSD) and silence prediction (PES) metrics. IDM demonstrates superior silence prediction capabilities compared to supervised baselines and achieves comparable LSD scores to LarsNet for most instruments except toms. Direct synthesis produces lower LSD values than masked outputs for all classes except cymbals, suggesting our generative approach can produce spectrally accurate reconstructions without the artifacts introduced by masking.

2) **Masking-based separation:** The results for masking-based separation are presented in Figure 7. The proposed IDM model outperforms all NMFD baselines by a substantial margin across all metrics, despite having access to transcription information during inference. Compared to the supervised LarsNet, our approach performs slightly worse on masked metrics, though we outperform the LarsNet Mono configuration on LSD.

According to the nSDR scores, a notable challenge appears in separating Cymbals and Hi-Hats, where the fixed one-shot duration of 1 second in our approach might be insufficient to model their longer decay characteristics [15], negatively affecting objective metrics without necessarily reflecting perceptual quality.

3) **Influence of onsets during inference:** Including ground-truth onsets during inference (IDM+ onsets) consistently improves separation performance, occasionally surpassing LarsNet Mono or LarsNet results (e.g., on kick for masked LSD and Hi-Hats for synth LSD). This is very noticeable for Toms in the train kits and for Hi-Hats and Cymbals for the test kits.. This confirms that our method’s optimal performance depends on accurate onset detection, though the relatively small improvement margin reflects our model’s already strong transcription capabilities.

4) **Test kits:** Even though IDM has only been trained to synthesize 6 drum kits, it still produces reasonable results

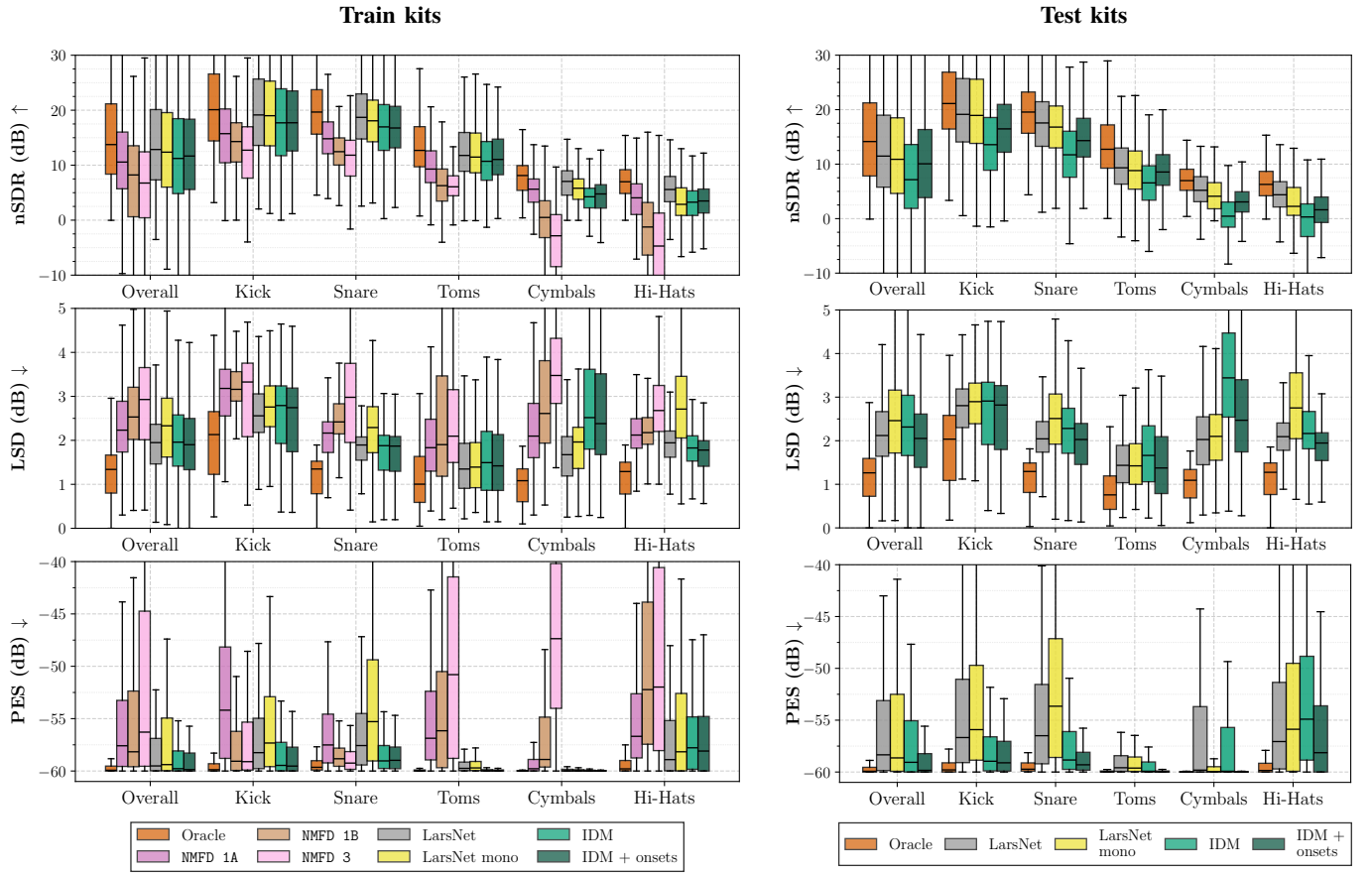


Fig. 7. Comparison of masking-based separation performance metrics on the full test set of StemGMD. The left column shows results on drum kits used during training and the right column shows results on test kits. From top to bottom, the plots display Signal-to-Distortion Ratio (higher is better), Log Spectral Distance (lower is better), and Predicted Energy in Silence (lower is better) for masked outputs.

when prompted to separate the 4 held-out test kits. While there's significant spectral overlap between the different drum instruments, different samples from the same class share high spectral similarity and thus masking-based separation (Figure 7, right) and synthesis-based spectral distance (Figure 6, right) yield comparable, and sometimes better results than the strongest baselines.

5) **Results in 9-class configuration:** We report model results in the full 9-Class configuration in Table III for reference. The 9-Class configuration provides a more detailed view of the model's performance across all drum instruments. Particularly notable is the disparity between open and closed hi-hats, which are often grouped in evaluation protocols such as that used by [6].

## V. DISCUSSION

Our experimental results demonstrate that the proposed IDM approach successfully integrates transcription and synthesis for Drum Source Separation. Without requiring access to ground-truth isolated stems during training, our model achieves performances comparable to the ones of supervised approaches that depend on such data while using  $\approx 100$  times less parameters (542.1K vs 49.1M). In addition, while datasets with clean, multitrack drum stems are scarce and challenging to produce, numerous datasets suitable for ADT are available,

TABLE III  
PERFORMANCE METRICS BY INSTRUMENT CLASS

Class	Masked			Synthesized	
	nSDR↑	LSD↓	PES↓	LSD↓	PES↓
kick	17.47	2.58	-54.37	1.84	-55.46
snare	17.29	1.73	-57.20	1.83	-58.87
hihat_closed	1.66	1.90	-55.88	1.94	-56.83
hihat_open	6.68	1.71	-59.81	1.86	-59.99
hi_tom	8.50	1.16	-59.57	1.03	-59.85
mid_tom	6.41	1.11	-59.62	0.90	-59.70
low_tom	7.35	1.62	-59.30	1.32	-59.57
ride	2.12	2.09	-59.57	2.24	-59.65
crash_left	4.78	2.84	-59.88	2.99	-59.94

ranging from large-scale MIDI-aligned collections to smaller, manually annotated corpora of real-world recordings, making our method scalable. The ability to directly synthesize one-shot samples for each instrument represents an additional advantage, facilitating potential applications in music production and remixing scenarios.

The transcription component can be improved by leveraging more data, state-of-the-art techniques [23], data augmentation [20], [22], incorporating beat information [19], and increasing the temporal resolution of onset detection. External ADT models or even human input could be integrated to enhance separation results in practical applications.

Our evaluation protocol reveals limitations in traditional DSS assessment methods. Waveform metrics exhibit considerable variance across instrument classes, suggesting they may not optimally measure objective performance. The 9-class results indicate significant performance disparities that challenge conventional class groupings, as exemplified by open hi-hats showing greater acoustic similarity to ride cymbals than to closed hi-hats. Finally, the sparsity of less frequently played instruments can bias track-level metrics due to the predominance of silence.

This approach could benefit musical traditions with significant percussive components, such as African or Latin American music [55], particularly in low-resource contexts where isolated stem data is scarce or unavailable.

## VI. CONCLUSION

This paper presents the Inverse Drum Machine (IDM), a novel approach to Drum Source Separation (DSS) that integrates Automatic Drum Transcription and One-shot drum Sample Synthesis in an end-to-end framework. By leveraging an analysis-by-synthesis methodology, our approach achieves high-quality DSS by replacing the need for isolated stems with more easily obtainable transcription data.

Experimental results demonstrate that IDM performs comparably to state-of-the-art supervised methods that require multitrack training data, while significantly outperforming matrix decomposition baselines. The modular synthesis framework and the ability to directly synthesize one-shot samples for each drum instrument provide additional flexibility for creative applications.

Future work may explore extending this approach to more diverse datasets and enhancing synthesis quality. The successful conditional synthesis without exposure to ground-truth isolated targets enables potential applications with more diverse drum kits and real-world drum mixture data. Future implementations could replace the one-hot representation of drum kits with pre-trained embedding models or learned representations. IDM could also potentially operate without transcription information by leveraging unsupervised learning approaches [13], while synthesis quality could be enhanced through adversarial learning techniques [30].

## ACKNOWLEDGMENTS

This work was funded by the European Union (ERC, HI-Audio, 101052978). Views and opinions expressed are however those of the author(s) only and do not necessarily reflect those of the European Union or the European Research Council. Neither the European Union nor the granting authority can be held responsible for them.

## REFERENCES

- [1] D. Fitzgerald, “Automatic drum transcription and source separation,” Ph.D. dissertation, Dublin Institute of Technology, Dublin, Ireland, 2004.
- [2] C. Dittmar and D. Gärtner, “Real-time transcription and separation of drum recordings based on NMF decomposition,” in *Proc. Int. Conf. Digit. Audio Effects*, 2014, pp. 187–194.
- [3] O. Gillet and G. Richard, “ENST-Drums: An extensive audio-visual database for drum signals processing,” in *Proc. Int. Soc. Music Inf. Retrieval Conf.*, 2006, pp. 156–159.
- [4] ———, “Transcription and separation of drum signals from polyphonic music,” *IEEE/ACM Trans. Audio Speech Lang. Process.*, vol. 16, no. 3, pp. 529–540, 2008.
- [5] C. Dittmar and M. Müller, “Reverse engineering the amen break - score-informed separation and restoration applied to drum recordings,” *IEEE/ACM Trans. Audio Speech Lang. Process.*, vol. 24, no. 9, pp. 1535–1547, 2016.
- [6] A. I. Mezza, R. Giampiccolo, A. Bernardini, and A. Sarti, “Toward deep drum source separation,” *Pattern Recognition Letters*, vol. 183, pp. 86–91, 2024.
- [7] T. D. Rossing, *Science of Percussion Instruments*. Singapore: World Scientific, 2000, vol. 3.
- [8] R. Hennequin, A. Khelif, F. Voituret, and M. Moussallam, “Spleeter: A fast and efficient music source separation tool with pre-trained models,” *J. Open Source Softw.*, vol. 5, no. 56, p. 2154, 2020.
- [9] A. Défossez, “Hybrid spectrogram and waveform source separation,” in *Proc. ISMIR Workshop Music Source Separation*, 2021.
- [10] A. I. Mezza, R. Giampiccolo, A. Bernardini, and A. Sarti, “Benchmarking music demixing models for deep drum source separation,” in *Proc. IEEE Int. Symp. Internet Sounds*. Erlangen, Germany: IEEE, 2024, pp. 1–6.
- [11] E. Manilow, P. Seetharaman, and B. Pardo, “Simultaneous separation and transcription of mixtures with multiple polyphonic and percussive instruments,” in *Proc. IEEE Int. Conf. Acoust. Speech Signal Process.* Barcelona, Spain: IEEE, 2020, pp. 771–775.
- [12] K. W. Cheuk, Y.-J. Luo, E. Benetos, and D. Herremans, “The effect of spectrogram reconstruction on automatic music transcription: An alternative approach to improve transcription accuracy,” in *Proc. Int. Conf. Pattern Recognit.* Milan, Italy: IEEE, 2020, pp. 9091–9098.
- [13] K. Choi and K. Cho, “Deep unsupervised drum transcription,” in *Proc. Int. Soc. Music Inf. Retrieval Conf.*, Delft, Netherlands, 2019, pp. 183–191.
- [14] K. Schulze-Forster, G. Richard, L. Kelley, C. S. Doire, and R. Badeau, “Unsupervised music source separation using differentiable parametric source models,” *IEEE/ACM Trans. Audio Speech Lang. Process.*, vol. 31, pp. 1276–1289, 2023.
- [15] L. Vande Veire, C. De Boom, and T. De Bie, “Sigmoidal NMF: Convolutional NMF with saturating activations for drum mixture decomposition,” *Electronics*, vol. 10, no. 3, p. 284, 2021.
- [16] J. Shier, F. Caspe, A. Robertson, M. Sandler, C. Saitis, and A. McPherson, “Differentiable modelling of percussive audio with transient and spectral synthesis,” in *Proc. Forum Acusticum*, 2023.
- [17] C.-W. Wu, C. Dittmar, C. Southall, R. Vogl, G. Widmer, J. Hockman, M. Müller, and A. Lerch, “A review of automatic drum transcription,” *IEEE/ACM Trans. Audio Speech Lang. Process.*, vol. 26, no. 9, pp. 1457–1483, 2018.
- [18] H. Lindsay-Smith, S. McDonald, and M. Sandler, “Drumkit transcription via convolutive NMF,” in *Proc. Int. Conf. Digit. Audio Effects*, York, UK, 2012.
- [19] R. Vogl, M. Dorfer, G. Widmer, and P. Knees, “Drum transcription via joint beat and drum modeling using convolutional recurrent neural networks,” in *Proc. Int. Soc. Music Inf. Retrieval Conf.*, Suzhou, China, 2017, pp. 150–157.
- [20] L. Callender, C. Hawthorne, and J. Engel, “Improving perceptual quality of drum transcription with the expanded groove MIDI dataset,” *arXiv preprint arXiv:2004.00188*, 2020.
- [21] R. Vogl, G. Widmer, and P. Knees, “Towards multi-instrument drum transcription,” in *Proc. Int. Conf. Digit. Audio Effects*, Aveiro, Portugal, 2018, pp. 57–64.
- [22] M. Zehren, M. Alunno, and P. Bientinesi, “High-quality and reproducible automatic drum transcription from crowdsourced data,” *Signals*, vol. 4, no. 4, pp. 768–787, 2023.
- [23] P. Weber, C. Uhle, M. Müller, and M. Lang, “Real-time automatic drum transcription using dynamic few-shot learning,” in *Proc. IEEE Int. Symp. Internet Sounds*. Erlangen, Germany: IEEE, 2024, pp. 1–8.
- [24] P. R. Cook, “Physically informed sonic modeling (PhISM): Percussive synthesis,” in *Proc. Int. Comput. Music Conf.*, 1996, pp. 228–231.
- [25] H. Han and V. Lostanlen, “Wav2shape: Hearing the shape of a drum machine,” in *Proc. Forum Acusticum*, 2020, pp. 647–654.
- [26] J. O. S. III and X. Serra, “PARSHL: An analysis/synthesis program for non-harmonic sounds based on a sinusoidal representation,” in *Proc. Int. Comput. Music Conf.*, 1987.
- [27] T. S. Verma and T. H.-Y. Meng, “Extending spectral modeling synthesis with transient modeling synthesis,” vol. 24, no. 2, pp. 47–59, 2000.
- [28] A. Ramires, P. Chandra, X. Favory, E. Gómez, and X. Serra, “Neural Percussive Synthesis Parameterised by High-Level Timbral Features,”

in *Proc. IEEE Int. Conf. Acoust. Speech Signal Process.* Barcelona, Spain: IEEE, 2020, pp. 786–790.

[29] C. Aouameur, P. Esling, and G. Hadjeres, “Neural drum machine : An interactive system for real-time synthesis of drum sounds,” in *Proc. Int. Conf. Comput. Creativity*, 2019, pp. 92–99.

[30] J. Nistal, S. Lattner, and G. Richard, “DRUMGAN: Synthesis of drum sounds with timbral feature conditioning using generative adversarial networks,” in *Proc. Int. Soc. Music Inf. Retrieval Conf.*, Utrecht, Netherlands, 2020, pp. 590–597.

[31] J. Drysdale, M. Tomczak, and J. Hockman, “Adversarial synthesis of drum sounds,” in *Proc. Int. Conf. Digit. Audio Effects*, Vienna, Austria, 2020, pp. 167–172.

[32] S. Rouard and G. Hadjeres, “CRASH: Raw audio score-based generative modeling for controllable high-resolution drum sound synthesis,” in *Proc. Int. Soc. Music Inf. Retrieval Conf.*, 2021, pp. 579–585.

[33] R. Simionato and S. Fasciani, “Sines, transient, noise neural modeling of piano notes,” *Frontiers in Signal Processing*, vol. 4, p. 1494864, 2025.

[34] P. Smaragdis, “Non-negative matrix factor deconvolution; extraction of multiple sound sources from monophonic inputs,” in *Proc. Intl. Conf. on Independent Component Analysis and Blind Signal Separation*. Grenada, Spain: Springer, 2004, pp. 494–499.

[35] C.-Y. Cai, Y.-H. Su, and L. Su, “Dual-channel drum separation for low-cost drum recording using non-negative matrix factorization,” in *Proc. Asia-Pacific Signal Inf. Process. Assoc. Annu. Summit Conf.* Tokyo, Japan: IEEE, 2021, pp. 17–22.

[36] J. Gillick, A. Roberts, J. Engel, D. Eck, and D. Bamman, “Learning to groove with inverse sequence transformations,” in *Proc. Int. Conf. Mach. Learning*, Long Beach, USA, 2019, pp. 2269–2279.

[37] J. H. Engel, L. Hantrakul, C. Gu, and A. Roberts, “DDSP: Differentiable digital signal processing,” in *Proc. Int. Conf. Learn. Representations*, 2020.

[38] N. Masuda and D. Saito, “Synthesizer sound matching with differentiable DSP.” in *Proc. Int. Soc. Music Inf. Retrieval Conf.*, 2021, pp. 428–434.

[39] B. Torres, G. Peeters, and G. Richard, “Unsupervised harmonic parameter estimation using differentiable DSP and spectral optimal transport,” in *Proc. IEEE Int. Conf. Acoust. Speech Signal Process.* Seoul, South Korea: IEEE, 2024, pp. 1176–1180.

[40] B. Hayes, J. Shier, G. Fazekas, A. McPherson, and C. Saitis, “A review of differentiable digital signal processing for music and speech synthesis,” *Frontiers in Signal Processing*, vol. 3, p. 1284100, 2024.

[41] M. Kawamura, T. Nakamura, D. Kitamura, H. Saruwatari, Y. Takahashi, and K. Kondo, “Differentiable digital signal processing mixture model for synthesis parameter extraction from mixture of harmonic sounds,” in *Proc. IEEE Int. Conf. Acoust. Speech Signal Process.* Singapore, Singapore: IEEE, 2022, pp. 941–945.

[42] G. Richard, P. Chouteau, and B. Torres, “A fully differentiable model for unsupervised singing voice separation,” in *Proc. IEEE Int. Conf. Acoust. Speech Signal Process.* Seoul, South Korea: IEEE, 2024, pp. 946–950.

[43] Z. Liu, H. Mao, C.-Y. Wu, C. Feichtenhofer, T. Darrell, and S. Xie, “A ConvNet for the 2020s,” in *Proc. IEEE/CVF Conf. Comput. Vis. Pattern Recognit.* New Orleans, USA: IEEE, 2022, pp. 11966–11976.

[44] C. Hawthorne, E. Elsen, J. Song, A. Roberts, I. Simon, C. Raffel, J. H. Engel, S. Oore, and D. Eck, “Onsets and frames: Dual-objective piano transcription,” in *Proc. Int. Soc. Music Inf. Retrieval Conf.*, E. Gómez, X. Hu, E. Humphrey, and E. Benetos, Eds., Paris, France, 2018, pp. 50–57.

[45] E. Perez, F. Strub, H. de Vries, V. Dumoulin, and A. Courville, “FiLM: Visual Reasoning with a General Conditioning Layer,” *arXiv preprint arXiv:1709.07871*, no. arXiv:1709.07871, 2017.

[46] A. Liutkus and R. Badeau, “Generalized Wiener filtering with fractional power spectrograms,” in *Proc. IEEE Int. Conf. Acoust. Speech Signal Process.* Brisbane, Australia: IEEE, 2015, pp. 266–270.

[47] J. L. Ba, J. R. Kiros, and G. E. Hinton, “Layer normalization,” *arXiv preprint arXiv:1607.06450*, 2016.

[48] S. Böck, F. Krebs, and M. Schedl, “Evaluating the online capabilities of onset detection methods,” in *Proc. Int. Soc. Music Inf. Retrieval Conf.*, Porto, Portugal, 2012, pp. 49–54.

[49] X. Wang, S. Takaki, and J. Yamagishi, “Neural source-filter waveform models for statistical parametric speech synthesis,” *IEEE/ACM Trans. Audio Speech Lang. Process.*, vol. 28, pp. 402–415, 2019.

[50] P. López-Serrano, C. Dittmar, Y. Özer, and M. Müller, “NMF toolbox: Music processing applications of nonnegative matrix factorization,” in *Proc. Int. Conf. Digit. Audio Effects*, vol. 19, 2019, pp. 2–6.

[51] C. Raffel, B. McFee, E. J. Humphrey, J. Salamon, O. Nieto, D. Liang, and D. P. W. Ellis, “MIR\_EVAL: A transparent implementation of common MIR metrics,” in *Proc. Int. Soc. Music Inf. Retrieval Conf.*, Taipei, Taiwan, 2014, pp. 367–372.

[52] Y. Mitsuishi, G. Fabbro, S. Uhlich, and F.-R. Stöter, “Music demixing challenge2021,” *arXiv preprint arXiv:2108.13559*, 2021.

[53] M. Torcoli, T. Kastner, and J. Herre, “Objective Measures of Perceptual Audio Quality Reviewed: An Evaluation of Their Application Domain Dependence,” *IEEE/ACM Trans. Audio Speech Lang. Process.*, vol. 29, pp. 1530–1541, 2021.

[54] K. Schulze-Forster, C. S. J. Doire, G. Richard, and R. Badeau, “Weakly informed audio source separation,” in *Proc. IEEE Workshop Appl. Signal Process. Audio Acoust.* IEEE, 2019, pp. 273–277.

[55] L. Maia, P. D. de Tomaz Jr., M. Fuentes, M. Rocamora, L. W. P. Biscainho, M. V. M. da Costa, and S. Cohen, “A novel database of brazilian rhythmic instruments and some experiments in computational rhythm analysis,” in *Proc. Audio Eng. Soc. Latin Amer. Conf.*, Montevideo, Uruguay, 2018.